

Vibrio deploys Type 2 secreted lipase to esterify cholesterol with host fatty acids and mediate cell egress

Marcela de Souza Santos^{1#}, Suneeta Chimalapati^{1,2#}, Ann Ray³, Wan-Ru Lee⁴,
Giomar Rivera-Cancel⁵, Alexander Lafrance¹, Gonçalo Vale⁶, Krzysztof Pawłowski⁷,
Matt Mitsche^{6,8}, Jeffrey G McDonald^{6,8}, Jen Liou⁴ & Kim Orth^{1,2,5*}

¹Department of Molecular Biology, University of Texas Southwestern Medical
Center, Dallas, TX 75390, USA

²Howard Hughes Medical Institute, University of Texas Southwestern Medical
Center, Dallas, TX 75390, USA

³Department of Microbiology, University of Texas Southwestern Medical Center,
Dallas, TX 75390, USA

⁴Department of Physiology, University of Texas Southwestern Medical Center,
Dallas, TX 75390, USA

⁵Department of Internal Medicine, University of Texas Southwestern Medical Center,
Dallas, TX 75390, USA

⁶Center for Human Nutrition, University of Texas Southwestern Medical Center,
Dallas, TX 75390, USA

⁷Faculty of Agriculture and Biology, Warsaw University of Life Sciences, Warsaw
02-776, Poland

⁸Department of Molecular Genetics, University of Texas Southwestern Medical Center,
Dallas, TX 75390, USA

[#]Both authors contributed equally to this work

*Correspondence: kim.orth@utsouthwestern.edu

Abstract

Pathogens find diverse niches for survival inside host cells where replication occurs in a relatively protected environment. *Vibrio parahaemolyticus*, a facultative intracellular pathogen, uses its type 3 secretion system 2 (T3SS2) to invade and replicate inside host cells. However, after extensive analysis, the T3SS2 pathogenicity island appeared to lack a mechanism for egress of this bacterium from the invaded host cell. Using a combination of cell biology, microbial genetics and lipid biochemistry, we found that VPA0226, a constitutively secreted lipase, is required for escape of *Vibrio parahaemolyticus* from host cells. Remarkably, this lipase must be delivered into the host cytoplasm where it preferentially uses fatty acids associated with innate immune response (i.e. arachidonic acid, 20:4) to esterify cholesterol, weakening the plasma membrane and allowing egress of the bacteria. This study reveals the resourcefulness of microbes and the interplay between virulence systems to evolve an ingenious scheme for survival and escape.

Impact Statement

Considering the course of a pathogen's evolution, there appears to be interplay between secretion systems, providing unique, synergistic mechanisms to support a successful lifestyle for possibly pathogenesis, symbiosis and/or parasitosis.

Main Text

As intracellular pathogens acquire mechanisms to invade a host cell, correlating mechanisms must also evolve for survival within the host and escape from the host. For example, the facultative intracellular pathogen *Vibrio parahaemolyticus* (*V. para.*) is a Gram-negative bacterium that resides in warm estuarine environments with some strains acquiring virulence factors that can cause illness, even death in animals including shrimp and humans (1). This pathogen can cause acute gastroenteritis due to the consumption of contaminated, undercooked seafood and possibly septicemia when infecting open wounds (1). *V. para.* contains a number of virulence factors, including hemolysins and two Type 3 Secretion Systems (T3SS1 and T3SS2) (2). Previous studies have shown that the more ancient T3SS1 is associated with all strains of *V. para.*, whereas T3SS2, a more recent acquisition, correlates with clinical isolates and disease in humans (2). To study the various virulence factors independently, deletions in particular genes are created to unmask the activity of a specific virulence mechanism (3). Herein, to study T3SS2, we utilize CAB2, a strain derived from the clinical isolate RIMD2210633 that is deleted for hemolysins and the T3SS1 (4).

The T3SS2 found on a pathogenicity island encodes a needle-like apparatus and effectors that mediate an invasive infection resulting in death of a host cell (5,6). T3SS2 translocates the effector VopC, a deamidase, to mediate membrane ruffling and uptake of *V. para.* by nonphagocytic cells (4,6). Once inside, *V. para.* escapes from an acidified endocytic compartment and proceeds to replicate in the cytoplasm of the host cell, reaching counts of 200-300 bacteria per host cell (6). Other translocated effectors have been shown to manipulate host cell signaling, including the acetyltransferase VopA that blocks MAPK signaling and the actin assembly factor VopL that blocks production of reactive oxygen species (7-10). *V. para.* ultimately escapes from this protective replicative niche to infect other cells (6). In total, about a dozen T3SS2 effectors are

thought to be delivered to the host cell, some with known molecular functions but with exception of the aforementioned effectors, understudied for their role in bacterial intracellular survival (3). After perusal of this pathogenicity island, there appeared to be no obvious candidate effector that would mediate the escape of *V. para.* from the endocytic compartment or the host cell.

Herein, we describe the identity of a lipase, VPA0226, which is necessary for egress of *V. para.* from the host cells. However, VPA0226 is not secreted by the T3SS2, rather it is constitutively secreted by type 2 secretion system. Using lipidomic studies we found that, unlike other bacterial lipases, VPA0226, but not its catalytically inactive forms (VPA0226-H/A or VPA0226-C/A), prefers to esterify cholesterol using host polyunsaturated fatty acids (PUFA), specifically those implicated in immune signaling. Esterification of cholesterol leads to a weakened plasma membrane that allows *V. para* to escape. This study exemplifies the resourcefulness and adaptability of bacteria to leverage existing mechanism to survive and escape from a host cell.

Results

The catalytic activity of VPA0226 is required for *V. para* egress from host cell.

Intracellular pathogens are known to use lipases to escape from membrane compartments, such as *Salmonella* spp. that require the T3SS lipase SseJ to escape from the *Salmonella* containing vacuole (11,12). Using SseJ as a probe in a bioinformatic search of the *V. para.* genome, we identified a lipase (VPA0226) with approximately 16% sequence identity and conservation of catalytic residues (**Figure 1-figure supplement 1A**). Previously, *in vitro* studies demonstrated that VPA0226 has lipase activity and structural studies on a related *Vibrio vulnificus* lipase revealed a chloride dependent catalytic diad (13,14). However, analysis of VPA0226 reveals a more classic catalytic triad of Ser-His-Asp (**Figure 1-figure supplement 1B**).

To test whether VPA0226 plays a critical role in *V. para*'s intracellular lifecycle, we performed a gentamicin protection assay, whereby cells are infected with the *V. para* CAB2 strain for 2 hours to allow invasion of the host and then treated with gentamicin

for the remainder of the infection to kill all extracellular, but not intracellular bacteria (6). We observed that the *V. para*. CAB2 containing a functional T2SS2 can efficiently invade, replicate (indicated by the increase in CFU counts), and escape from the host cell (indicated by the after-peak decrease in CFU counts due to exposure of egressed bacteria to gentamicin) (**Figure 1A, black bars**). By contrast, a CAB2 strain deleted for *vpa0226* (CAB2 Δ *vpa0226*) results in cells that have increasing amounts of bacteria with no significant decrease for up to 7 hours post gentamicin treatment (PGT), indicating the inability of these bacteria to escape from an invaded cell (**Figure 1A, green bars**).

To test whether cell egress was attributed to VPA0226's catalytic activity, we complemented the CAB2 Δ *vpa0226* with a wildtype copy of VPA0226 (CAB2 Δ *vpa0226*+WT) or with a catalytically inactive copy of VPA0226 (CAB2 Δ *vpa0226*+S/A). While *in-trans* complementation with a wildtype copy of VPA0226 allowed for bacterial escape, the catalytically inactive form of VPA0226 did not allow for egress of *V. para* from the host cell. (**Figure 1B**). Furthermore, the decrease in number of lysed host cells, as well as the decreased number of egressed mutant bacteria at 7 hours PGT in comparison to its parental strain is consistent with these findings (**Figure 1-figure supplement 1C and D, respectively**). We next turned to confocal microscopy and observed over the course of an infection (1, 3, 7 hours) that all CAB2 strains escape from the endocytic vacuole and replicate in the cytoplasm (**Figure 1-figure supplement 1E and F**). However, only CAB2 and CAB2 Δ *vpa0226*+WT, but not CAB2 Δ *vpa0226* and CAB2 Δ *vpa0226*+S/A, escape from the host cell after 7 hours PGT (**Figure 1C and Figure 1-figure supplement 1F**). These results support the previous observation that, in the absence of VPA0226, bacteria are unable to egress from its host cell.

VPA0226 is secreted by the type 2 secretion system

We speculated that VPA0226 is translocated as a T3SS effector, as it appears that VPA0226 is essential for *V. para*'s egress from the host cell when the bacterium uses a T3SS2-dependent mechanism to invade such cell (4). To test this hypothesis, we followed the secretion of VPA0226 from various *V. para* strains, including CAB2,

CAB2 Δ *vpa0226*, CAB3 (a strain that only contains the T3SS1), and CAB4 (a strain that contains neither T3SS1 nor T3SS2). To our surprise, with the exception of the CAB2 Δ *vpa0226* strain, we observed VPA0226 to be constitutively secreted from all of these *V. para* strains (**Figure 1-figure supplement 2A**). Further bioinformatic analysis using SignalP5.0 revealed that VPA0226 contained a signal peptide at its N-terminus similar to those found for enzymes that are secreted out of the type 2 secretion system (15) (**Figure 1-figure supplement 2B**). To test whether VPA0226 is secreted through this system, we assayed the following strains for VPA0226 secretion: CAB2; CAB2 Δ *vpa0226*; a CAB2 strain deleted for EpsD (an essential type 2 secretion system outer membrane component), CAB2 Δ *epsD*; and the EpsD complemented strain CAB2 Δ *epsD*+EpsD. We observed that VPA0226 is secreted by CAB2 and CAB2 Δ *epsD*+EpsD, but not by CAB2 Δ *vpa0226* or CAB2 Δ *epsD*, thereby demonstrating that VPA0226 is secreted by the type 2 secretion system (**Figure 1D, Figure 1-figure supplement 2C**).

Intracellular VPA0226 associates with and disrupts membranes of invaded cells.

Since VPA0226 is predicted to be a lipase that hydrolyses fatty acids of phospholipids and can transfer fatty acids to cholesterol, we speculated that VPA0226 would be associated with a host membrane. We expected VPA0226 would associate with the plasma membrane as it appears to be involved in bacterial egress from the host cell through this membrane. To test this hypothesis, we transiently transfected VPA0226 tagged with GFP (VPA0226-GFP) into HeLA cells and observed that cells expressing VPA0226-GFP died within 24 hours (data not shown); however, at an earlier time point (14 hours), the transfected cells were viable. Somewhat perplexing, VPA0226-GFP was not localized to the plasma membrane but to an intracellular membrane compartment (**Figure 2A**). To assess which compartment this might be, we co-stained transfected cells with markers for a number of intracellular compartments, including early endosomes using EEA1, late endosomes/lysosomes using Lamp-1, endoplasmic reticulum using calnexin and mitochondria using Acetyl-CoA acetyl transferase (ACAT1) and COXIV (**Figure 2, Figure 2-figure supplement 1A,B,C,D**). The only markers co-staining with VPA0226 were ACAT1 and COXIV, indicating that VPA0226 associates

with the mitochondria (**Figure 2A, figure 2-figure supplement 1D**). In addition, while mitochondria of cells mock-transfected or transfected with the catalytically inactive VPA0226 (VPA0226-H/A) show normal cell morphology, cells transfected with the wildtype VPA0226 display fragmented mitochondria (**Figure 2A, figure 2-figure supplement 1D**).

The changes in morphology of the mitochondria also occurred during infection, as host cells invaded with the CAB2 strain revealed similar fragmented mitochondria at approximately 2 hours PGT (**Figure 2B, Figure 2-figure supplement 1E,F**). Cells that do not contain bacteria appear to have normal mitochondria (**Figure 2B, Figure 2-figure supplement 1E,F**). In addition, cells infected with CAB2 Δ vpa0226 strain exhibit normal mitochondrial morphology throughout the infection (**Figure 2B-figure supplement 1E**). Consistent with the transfection studies, mitochondrial fragmentation was dependent on the intact catalytic activity of VPA0226 (**Figure 2B, figure supplement 1E,F**). As we only saw changes in mitochondria when VPA0226 is provided by an intracellular source (invaded or transfected cells), we conclude that VPA0226 must be supplied intracellularly to cause changes in the mitochondria.

***V. para*-initiated apoptosis is not required for bacterial cell egress**

Based on these studies, we made the supposition that disrupting lipids in the mitochondrial membrane causes fragmentation of this membrane and compromises the integrity of this compartment resulting in cytochrome C release and the initiation of apoptosis. However, the initiation of these events would not support a mechanism for egress of *V. para* from the host cell as apoptosis does not result in lysis or release of intracellular contents. Instead, if VPA0226 would compromise the cellular membranes by esterifying cholesterol, the integrity of all membranes would be compromised, including the plasma membrane, thereby allowing the escape of *V. para* from host cells.

To address these hypotheses, we analyzed apoptotic signaling in host cells during infection. Since mitochondria are fragmented at 2 hours PGT, we tested whether Cytochrome C, an initiator of apoptosis, is released from the mitochondria at some point after this. Consistent with this idea, we observed the release of Cytochrome C into the cytoplasm in CAB2 and CAB2Δvpa0226+WT infected cells, but not CAB2Δvpa0226 and CAB2Δvpa0226+S/A infected cells (**Figure 2-figure supplement 2A,B**) by 5 hours PGT.

Based on the observations that Cytochrome C is released, we expected to observe downstream indicators of apoptosis, such as fragmented DNA. Indeed, we observed positive TUNEL staining in CAB2 and CAB2Δvpa0226+WT infected cells but not in CAB2Δvpa0226 and CAB2Δvpa0226+S/A infected cells after 5 hours PGT (**Figure 2-figure supplement C,D**). Interestingly, while treatment of cells with an inhibitor of apoptosis Z-VAD-FMK did inhibit apoptosis in staurosporine treated cells, Z-VAD-FMK did not alter the progression of *V. para*-mediated invasion or the survival and escape of the CAB2 strains from the host cells (**Figure 2-figure supplement E,F**). Based on this observation, we propose that VPA0226-mediated fragmented mitochondria leads to the initiation of apoptosis. However, death by apoptosis is not a mechanism used for cell lysis because *V. para* escapes from the host cell 5 hours PGT whether or not apoptotic processes are active or inhibited (**Figure 2-figure supplement E**).

VPA0226 esterifies cholesterol using host polyunsaturated fatty acids

To address how VPA0226-mediated fragmentation of the mitochondria was occurring, we analyzed the lipase activity of VPA0226 and its impact on host cellular lipids during the course of infection. Previously, it was shown that lipases similar to VPA0226 can esterify cholesterol by the transfer of an acyl group from an acyl-containing lipid to cholesterol thereby converting free cholesterol to a cholesteryl ester (16,17). It should be noted that only the lipase activity, but not the transferase activity, has been observed previously for *Vibrio* lipases (14,18). To confirm lipase activity of VPA0226, we tested this enzyme with the EnzChek® Phospholipase A2 (PLA2) Assay Kit (Invitrogen). Purified wildtype VPA0226 but not the catalytically inactive VPA0226- S/A mutant

resulted in a concentration dependent increase in fluorescence from a PLA2 specific fluorogenic substrate (BODIPY PC-A2) (**Figure 3-figure supplement 1A**). We next assessed whether VPA0226 can directly modify cholesterol by incubating purified secreted wildtype or catalytically dead VPA0226- S/A with liposomes containing lipid mixtures of cardiolipin and cholesterol, followed by lipid extraction and thin layer chromatography. We observed that the wildtype but not the catalytically inactive VPA0226-S/A mutant facilitated the esterification of cholesterol (**Figure 3-figure supplement 1B**).

We next asked whether the expression of VPA0226 would change the global profile of esterified cholesterol in cells. To test whether VPA0226 alters lipids in cells, we transfected HeLa cells with an empty vector, wildtype VPA0226 and the catalytically inactive VPA0226-H/A mutant. At 14 hours post transfection (the same time point we observe changes in mitochondria (**Figure 3A**)), cells were harvested, total lipids were extracted and analyzed by thin layer chromatography (19). We observed a clear difference in the migration pattern of total lipids from VPA0226 WT transfected cells compared to those transfected with empty vector and the inactive VPA0226-H/A mutant. (**Figure 3, Figure 3-figure supplement 3C**). Based on these results we hypothesize that *in vivo* VPA0226 uses lipids to esterify cholesterol, resulting in changes in host cell membranes in the wildtype but not catalytically inactive VPA0226-H/A transfected cell. Because cellular membrane integrity is compromised when the levels of free cholesterol are reduced (20,21), these VPA0226-mediated changes are predicted to compromise the integrity of all host cell membranes, including the plasma membrane.

To assess which fatty acids are being used to esterify cholesterol, we performed lipidomic analysis of cells transfected for 14 hours with empty vector, VPA0226 and the catalytically inactive VPA0226-H/A. Since cardiolipin is a lipid found exclusively in mitochondria and bacterial outer membranes and VPA0226, a constitutively secreted lipase is localized to mitochondria, this enzyme might favor using fatty acids from cardiolipin (18:1,18:2,18:3) as a resource to esterify cholesterol. However, the levels of cholesteryl esters (CE) with cardiolipin fatty acids did not change significantly over the

three samples (**Figure 3B**). Rather, the cholesteryl esters that did dramatically change in the presence of wildtype VPA0226 included CE(20:3), CE(20:4), CE(20:5) and CE(22:6). Interestingly, these fatty acids are ones implicated with innate immune signaling, with the most notable being arachidonic acid (20:4) (22).

Increase in esterified cholesterol compromises the integrity of the plasma membrane.

We speculated that the dramatic increase in esterified cholesterol that correlated with the fragmented mitochondrial membranes would compromise the integrity of all cellular membranes, including the plasma membrane. To assess whether there was a decrease in free cholesterol, we tested whether the cellular sensor for free cholesterol, SREBP, was activated in cells transfected with VPA0226 (23). HeLa cells were transfected for 14 hours with empty vector, VPA0226 or the catalytically inactive VPA0226H/A and qPCR analysis was performed assessing genes that are targets of SREBP transcriptional activity. We observed all three genes, HMGCR, HMGCS and DHCR24, were upregulated in cells expressing VPA0226, but not in cells with the empty vector or the catalytically inactive VPA0226H/A (**Figure 4A**). These data support the proposal that cholesterol levels are being compromised in cells expressing VPA0226.

Next, we asked whether cells subjected to VPA0226 activity might be more fragile when subjected to mechanical stress, in this case we used osmotic stress. HeLa cells were transfected for 14 hours with empty vector, VPA0226 or the catalytically inactive VPA0226-H/A and then treated with water containing propidium iodide to assess their susceptibility to hypotonic stress. We observed that cells expressing VPA0226, but not in cells with the empty vector or the catalytically inactive VPA0226-H/A, lysed more readily as indicated by an increase in fluorescence (**Figure 4B**).

Finally, to further assess the integrity of the plasma membrane during infection, HeLa cells were infected with CAB2 strains and tested for permeability using Sytox, a stain that is only permeable to damaged membranes. We observe that cells infected with either CAB2 or CAB2 Δ vpa0226+WT, but not with CAB2 Δ vpa0226 and

CAB2Δ*vpa0226*+S/A, take up the Sytox stain at 5 hours PGT, indicating that their membranes have been compromised (**Figure 4C**). Furthermore, only cells that are invaded with *V. para* take up the sytox stain, consistent with the observation that only the invaded cells with an internal source of VPA0226 have compromised membranes.

Discussion

Intracellular bacteria must find mechanisms to invade, survive and escape the host cell. Previously, the mechanism of entry for *V. para* was discovered to be mediated by the deamidase activity of VopC (4). Further studies uncovered mechanisms used by *V. para* to attenuate signaling pathways inside the infected cell, by effectors such as VopA and VopL (3,9). Many other mechanisms remain to be elucidated for *V. para*'s defense against the host. Herein, we find that the escape route for *V. para* mediated host cell invasion is dependent on the Type 2 secreted lipase VPA0226 that compromises the integrity of the plasma membrane by using polyunsaturated fatty acids to esterify cholesterol in the infected cell. For this pathogen, VPA0226 provides an essential activity for the virulence of the T3SS2 pathogenicity island by providing a convenient mechanism for escape. When dissecting the activity mediated by VPA0226, we are struck by its many unconventional and somewhat perplexing properties, including its secretion, enzymology and biology.

VPA0226 is secreted, not by the T3SS2, but by the type 2 secretion system. These findings make it very clear that, although we attribute *V. para* virulence to T3SS2, this bacterial pathogen uses many tools outside of this pathogenicity island for a successful infection. Other tools would include external host signaling factors, such as bile salts for activation of the system and adhesion proteins used to attach to host cells (24,25).

VPA0226 appears to be constitutively secreted from *V. para* by the type 2 secretion system, as we saw no accumulation of VPA0226 inside *V. para* cells, indicating that, as it is synthesized it is secreted (**Figure1 - Figure supplement-2**). Additionally, when media is collected from log-phase *V. para* cultures, we are able to purify VPA0226 from

the culture medium. We propose that VPA0226 is constitutively secreted by intracellular bacteria during infection because we only observe changes in the mitochondria, release of cytochrome C, TUNEL positive cells and sytox membrane permeability in host cells that are invaded with *V. para* expressing wild type VPA0226. Therefore, VPA0226 targets host cell machinery from within the host cell and not from the outside.

With regards to its localization, we observe transfected VPA0226 localized to the mitochondria and during invasion of *V. para* and transfection of VPA0226, the mitochondria are fragmented. Neighboring cells that are not invaded or transfected appear to have mitochondria with a normal phenotype. Although we have been unable to detect VPA0226 during an infection, we propose using Koch's molecular postulate that the wildtype but not the catalytically inactive VPA0226 causes the fragmented mitochondrial phenotype (26). As VPA0226 does not appear to encode a mitochondrial localization domain, how and why it localizes specifically to the mitochondria is unclear.

Secreted phospholipases have been associated with many virulence activities, including mucus degradation, hemolysis and phagosome escape (27). These enzymes have broad substrate specificity and can work both as lipases and acyl transferases. Homologues of VPA0226 in *Vibrio* species such as *vhhA* in *V. harveyi*, *VvPlpA* in *V. vulnificus*, and *phlA* in *V. mimicus*, are implicated in virulence but have only been shown to possess the lipase activity (28-30). Recombinant VvhA from *Vibrio vulnificus* was shown to induce NF-κB-dependent mitochondrial cell death mediated by the production of lipid raft-dependent ROS (31). Another structural homologue *lec / VC_A0218* in *V. cholerae* with lipase activity is implicated in escape from the infected amoeba (18). In addition, a genetically non-homologous but functionally similar TgLCAT, lecithin: cholesterol acyltransferase encoded by a protozoan parasite *Toxoplasma gondii* is also implicated in host cell egress (32).

Using bioinformatics and clustering analysis, we find that VPA0226 is in a clan of enzymes containing invariant catalytic Ser, Gly, Asn and His residues which are referred to as GDSL-like lipases (33) (**Figure 1-figure supplement 1C**). VPA0226 and

homologs from other *Vibrio* species, together with the *Salmonella* phospholipase effector SseJ, are located in a mostly bacterial subfamily, closely related to plant and fungal GDSL lipases and only remotely related to animal GDSL lipases, e.g. human Phospholipase B1 (**Figure 3-figure supplement 1D**). Based on this conservation, we predict that the presence of VPA0226 in the *V. para* genome predated the acquisition of the T3SS2 pathogenicity island (2). From an evolutionary standpoint, it is interesting (and resourceful on the part of a bacterial pathogen) that this enzyme subsequently became an essential factor for escape of the invading *V. para*. Interestingly, the bacterial-plant-fungal GDSL lipase subfamily includes a large plant group of extracellular lipases (e.g. more than 100 different proteins in *Arabidopsis*), many of which are involved in regulation of defense against bacterial and fungal pathogens. Fungal members of the subfamily are found in most fungal lineages, including several pathogenic, but excluding yeast-like ones. Majority of this subfamily members are predicted to be secreted by possessing a classical signal peptide while a number of bacterial members additionally possess the autotransporter “translocator” domains (PMID: 21616712). This may suggest an alternative, speculative evolutionary scenario for this subfamily, involving horizontal gene transfers between pathogens and hosts. Our work confirms previous observations demonstrating that VPA0226 has lipase activity (**Figure3 - Figure supplement-2a**) (14). We went on to show both in vitro and in vivo VPA0226 can function as an acyl transferase. Interestingly, VPA0226 appears to act like a phospholipase A2 (PLA2) because using lipidomics, we observe that VPA0226 specifically transfers an acyl group from position 2 from the glycerol backbone of a phospholipid to cholesterol (34). The products from this reaction are esterified cholesterol and lysophospholipids, both of which destabilize membranes (35). The esterified cholesterol produced by VPA0226 are quite selective PUFAs, including 20:3, 20:4 (arachidonic acid) and 20:5 and 22:6 (fish oil lipids). This result was quite surprising for two reasons: first, the GDSL-like lipase from bacteria have been shown to use fatty acids (such as cardiolipin) as substrates as these are associated with bacteria; second, although eukaryotes produce cardiolipin, the substrate of choice for VPA0226 was clearly to use the aforementioned PUFAs to esterify cholesterol. Interestingly, these

PUFAs (arachidonic acid and fish oil lipids) are implicated with immune signaling (22,36).

From a biological perspective, we observe a well-timed, orchestrated escape of *V. para* from the host cell. VPA0226 is secreted into the host cytosol, localizing to the mitochondria and esterifying cholesterol over the course of about 5-6 hrs. During that time, *V. para* reaches a density of about 300 bacteria/invaded cell and, due to mechanical stress, egresses from the host cell. We observe that *V. para* uniquely utilizes two independent secretion systems to support its intracellular lifestyle. From the perspective of virulence, *V. para* appears to have utilized existing resources to evolve an efficient mechanism for invasion, propagation and escape. We speculate, considering the time pathogens have to evolve, that there is actually more interplay between secretion systems, providing unique, synergistic mechanisms to support a successful lifestyle of possibly pathogenicity, symbiosis and/or parasitosis.

Materials and Methods

Bacterial strains and culture conditions

The *V. parahaemolyticus* CAB2 strain was derived from POR1 (clinical isolate RIMD2210633 lacking TDH toxins), the latter being a generous gift from Drs. Tetsuya Iida and Takeshi Honda (4,37). The CAB2 strain was made by deleting the gene encoding the transcriptional factor ExsA, which regulates the activation of the T3SS1 (4,38). CAB2 was grown in Luria-Bertani (LB) medium, supplemented with NaCl to a final concentration of 3% (w/v), at 30 °C. When necessary, the medium was supplemented with 50 µg/mL spectinomycin (to select for growth of CAB2-GFP strains(39)) or 250 µg/mL kanamycin.

Antibodies

Antibodies were purchased from following companies. Rabbit polyclonal anti LAMP-1 – Abcam, mouse polyclonal anti-EEA1 and mouse monoclonal anti Cytochrome C – BD Biosciences, rabbit monoclonal anti COXIV and rabbit monoclonal anti calnexin – Cell Signaling Technologies, rabbit polyclonal anti ACAT1 – Genetex. Secondary antibodies

Alexa Fluor 647/568 goat anti-mouse/rabbit were obtained from Life Technologies, and Alexa Fluor 555 goat anti-mouse from Invitrogen. The antibody against VPA0226 was custom-made by Thermo Scientific.

Deletion of *vpa0226* and *epsD* from CAB2 strain

For in-frame deletion of *vpa0226* (GeneBank sequence accession number [NC_004605.1](#)), the nucleotide sequences 1kb upstream and downstream of the gene were cloned into pDM4, a Cm^r Ori6RK suicide plasmid (4). Primers used were 5' GATCGTCGACATCAAATTGAATGCACTATGATC 3' and 5' GATCACTAGTAAAGAAGACCCCTTTATTGATTC 3' for amplification of 1kb upstream region, and 5' GATCACTAGTCTAGCGAGCACATAAAAAGC 3' and 5' GATCAGATCTTCCGGGGTGGTAAATGCTT 3' for 1kb downstream region. 1kb sequences were then inserted between Sall and SpeI sites (upstream region) or SpeI and BglII (downstream region) sites of the plasmid multiple cloning site. For the deletion of *epsD*, the primers used were 5' GATCGTCGACATCAAATTGAATGCACTATGATC 3' and 5' GATCACTAGTAAAGAAGACCCCTTTATTGATTC 3' for amplification of 1kb upstream region, and 5' GATCACTAGTCTAGCGAGCACATAAAAAGC 3' and 5' GATCAGATCTTCCGGGGTGGTAAATGCTT 3' for 1kb downstream region. 1kb sequences were then inserted between Sall and SpeI sites (upstream region) or SpeI and BglII (downstream region) sites of the plasmid multiple cloning site. The resulting construct was inserted into CAB2 via conjugation by S17-1 (*λpir*) *Escherichia coli*. Transconjugants were selected for on minimal marine medium (MMM) agar containing 25 µg/mL chloramphenicol. Subsequent bacterial growth on MMM agar containing 15% (w/v) allowed for counter selection and curing of *sacB*-containing pDM4. Deletion was confirmed by PCR and sequencing analysis.

Complementation of CAB2Δ*vpa0226* and CAB2Δ*epsD*

For reconstitution of CAB2Δ*vpa0226*, the sequence coding for *vpa0226* was amplified using primers 5' GATCCTGCAGATGCTTAAAATTAAGTGCCT 3' and 5' GATGAATTCTTACTTATCGTCGTCATCCTTGTAATC 3' and then cloned into the pBAD/Myc-His vector (Invitrogen, resistance changed from ampicillin to kanamycin)

between PstI and EcoRI sites. For reconstitution of CAB2Δ*epsD* full length EpsD along with 1.2kb upstream region was amplified using primers 5' ATCGGAGCTCAGAACTACGCTATCTAATCACTG 3' and 5' ATCGGGTACCGTTCTTTTCCATTGATCGAT 3' and cloned into SacI and KpnI sites of pBAD/*Myc*-His vector. The resulting construct was inserted into CAB2Δ*vpa0226* or CAB2Δ*epsD* via triparental conjugation using *E. coli* DH5α (pRK2073). Transconjugants were selected for on MMM agar containing 250 µg/mL kanamycin. Reconstitution was confirmed by PCR. Empty pBAD plasmid (without *vpa0226/epsD* gene insertion) was introduced to CAB2 and or CAB2Δ*epsD* strains for consistency in bacterial strain manipulation. Expression of *vpa0226* was induced by bacterial culturing in the presence of 0.02% arabinose to activate pBAD's *araC* promoter and *EpsD* was expressed through its native promoter. For the expression of catalytically inactive VPA0226, a serine residue at position number 153 was modified to alanine through site directed mutagenesis using VPA0226pBAD/*Myc*-His vector as a template and primers 3' CCAACGTGAGCCACTGCGGAACAGACTATGTCCG 5' and 5' GGTGCACTCGGTGACGCCTTGTCTGATACAGGC 3'. The resulting construct was inserted into CAB2Δ*vpa0226* as detailed above.

T3SS2 and T2SS expression and secretion assay

For the expression and secretion of T3SS2, overnight grown *V. para.* strains in MLB at 30°C were diluted to OD600 of 0.3 in LB supplemented with 0.05% bile salts and grown at 37°C for 3h, as previously described (40). For the expression fraction, bacterial cultures of OD600 of 0.5 were pelleted and resuspended in 2x Laemmli buffer. For the secretion fraction, bacterial culture supernatants were filtered with a 0.22micron filter and precipitated with deoxycholate (150 µg/ml) and trichloroacetic acid (7% v/v). Precipitated proteins were pelleted, washed twice with acetone and then resuspended in 2x Laemmli buffer. Expression and secretion levels were detected by western blot analysis. Total protein load was assessed by staining the nitrocellulose membrane with coomassie blue or Ponceau. For T2SS expression and secretion, the same protocol was used except that the cultures were grown at 30°C in MLB without the addition of bile salts.

Lactate dehydrogenase (LDH) cytotoxicity assay

HeLa cells were plated in triplicate in a 24-well tissue culture plate at 7×10^4 cells per well and grown for 16-18h. Overnight grown bacterial cultures in MLB at 30°C were diluted to OD600 of 0.3 in MLB supplemented with 0.05% bile salts and grown at 37°C for 90 min to induce T3SS2. Induced *V. para.* cultures were then used to infect HeLa cells at MOI 10. Immediately after the addition of bacteria to HeLa cells plates were centrifuged for 5 min at 1000 rpm to synchronize infection. Gentamicin was added to HeLa cells at 100 µg /ml after 2h of infection. Seven hours post PGT, 200 µL of media from each well was transferred to a 96 well plate and centrifuged at 1000 rpm for 5 min, then 100 µL of this supernatant was used to evaluate LDH release into the culture medium as a measure of host cells lysis using a colorimetric cytotoxicity detection kit (Takara Bio) according to manufacturer's instructions. HeLa cells treated with 1% Triton X-100 for 10 min at the end of gentamicin treatment were used as positive control and cell lysis was expressed as a % of Triton treated cell lysis.

Gentamicin protection assay

Bacteria were added to triplicate wells of HeLa cell monolayers for infection as described in LDH assay. All infections were carried out at a MOI of 10. Gentamicin was added at 100µg/mL to each well after 2h of infection to kill extracellular bacteria. At each indicated time point, monolayers of HeLa cells were washed with PBS and cells were lysed by incubation with PBS containing 0.5% Triton X-100 for 10 min at room temperature with agitation. Serial dilutions of lysates were plated on MMM plates and incubated at 30 °C overnight for subsequent CFU enumeration. Z-VAD-FMK (EMD Millipore) was added to HeLa cells at the beginning of infection at 50µM where indicated. Z-VAD-FMK at this concentration prevented apoptotic cell-death induced by 1.2µM staurosporine (Abcam).

Immunofluorescence and confocal microscopy

HeLa cells were seeded onto 6-well plates containing sterile coverslips at a density of 7×10^4 cell/mL. Following infections with *V. para.* strains and indicated gentamicin

treatment times, cells were washed with PBS and fixed in 3.2% (v/v) para-formaldehyde for 10 min at room temperature. Fixed cells were washed in PBS and permeabilized with either 0.5% Triton X-100 in PBS (EEA1) or 0.5% saponin in PBS (LAMP1) for 4 min at room temperature(6). For calnexin, ACAT1, COXIV and Cyto C, fixed cells were permeabilized with ice cold methanol for 10 min at -20°C. After washing with PBS, blocking was performed with either 1% BSA (EEA1), 1%BSA with 0.1% saponin (LAMP1) or 5% normal goat serum with 0.3% Triton X-100 (calnexin, ACAT1, COXIV and Cyto C) for 30 minutes at room temperature. Primary and secondary antibodies were diluted in PBS containing either 0.5% BSA and 0.25% Tween 20 (EEA1), 0.5% BSA and 0.25% saponin (LAMP1) or 1% BSA and 0.3% Triton X-100 at appropriate dilutions and incubated serially for 1h at room temperature. Between each antibody incubation, coverslips were washed three times with PBS or PBS containing 0.1% saponin (LAMP1) for 5 min each wash. Nuclei and actin cytoskeleton were stained with Hoechst (Sigma) and rhodamine-phalloidin (Molecular Probes), respectively. For Sytox orange (Thermo Fisher Scientific) staining, cells were incubated with 0.5 µM Sytox orange for 15 min following infections with *V. para.* strains and gentamicin treatment. TUNEL staining was performed using DeadEnd fluorometric TUNEL system (Promega) according to manufacturer's instructions. Briefly, HeLa cells following infections and gentamicin treatment were fixed with 3.2% paraformaldehyde for 10 min at room temperature and permeabilized using 0.2% triton x 100 in PBS for 5 min at room temperature. Cells were then incubated with equilibration buffer for 10 min at room temperature followed by incubation with rTdT nucleotide mix at 37°C for 1h and nuclear staining with Hoechst. All imaging was performed on a Zeiss LSM 800 confocal microscope and images were converted using ImageJ (NIH).

Mammalian expression constructs + transfection

For mammalian cell expression, full length VPA0226 was amplified using primers 3' GATC AGATCT ATGATGAAAAACAATCACACTA 5' and 5' GATA GAATTC G GAAACGGTACTCGGCTAAGTTGTT 3' and cloned in frame with GFP into the expression vector sfGFP-N1 (41) (Addgene) between BglII and EcoRI sites for the expression of C terminally tagged VPA0226. Generating a catalytically inactive S153A

for this construct however, did not result in successful mammalian cell expression through transfection. Therefore, a second catalytically inactive C terminally tagged VPA0226 construct was then generated by subjecting the full-length plasmid to site directed mutagenesis to change a single amino acid residue histidine at 393 position to alanine using the primers 3' TGAGTTGCTGTTGTTGGAGCCGTGACATCCCAGAACAC 5' and 5' GTGTTCTGGGATGTCACGGCTCCAACAACAGCAACTCA 3'. For mammalian cell transfections HeLa or HEK293T cells were plated in 6-well plates containing sterile coverslips at 7×10^4 cell/ml or 2.5×10^5 cell/ml respectively and grown for 24h. Transient transfections were carried out for 16-20h with either 500 ng of construct DNA + 500 ng of pSFFV as filler using FugeneHD (Promega) or 1 μ g of construct DNA using Polyjet transfection reagent (Fisher Scientific) according to manufacturer's instructions.

Lipidomics

For lipidomics analysis, transfections were carried out following a previously described protocol (17). HeLa cells (3×10^6) were plated and transfected with 2 μ g of plasmids encoding VPA0226-WT sf-GFPN1 or VPA0226-H/A sf-GFPN1 using Polyjet transfection reagent according to manufacturer's instructions. 14h post transfection cells were washed 3 times with PBS and lipids were extracted from cell pellets following Bligh and Dyer's protocol using chloroform : methanol : 0.88% NaCl in 1:2:0.8 ratio (19). The extracted lipids were dissolved in 15 μ l of chloroform and processed for TLC analysis using plastic backed silica gel 60F254 plates (Sigma) and a mobile phase system containing petroleum ether: ethyl ether: acetic acid in 90:10:1 ratio. Lipid spots were visualized by exposure to iodine vapor. Cholesterol, cardiolipin (1',3'-bis[1,2-dioleoyl-sn-glycero-3-phospho]-glycerol), DOPS (1,2-dioleoyl-sn-glycero-3-phospho-L-serine) (Avanti Polar Lipids) and cholesteryl ester (cholesterol oleate, Sigma) were spotted as standards on the TLC plate.

Analysis of Lipids by LC-MS

All solvents were either HPLC or LC/MS grade and purchased from Sigma-Aldrich (St Louis, MO, USA). All lipid extractions were performed in 16 \times 100mm glass tubes with

PTFE-lined caps (Fisher Scientific, Pittsburg, PA, USA). Glass Pasteur pipettes and solvent-resistant plasticware pipette tips (Mettler-Toledo, Columbus, OH, USA) were used to minimize leaching of polymers and plasticizers.

Samples were transferred to glass tubes for liquid-liquid extraction (LLE) by modified Bligh/Dyer (42); 1mL each of dichloromethane, methanol, and water were added to the glass tube containing the sample. The mixture was vortexed and centrifuged at 2671 $\times g$ for 5 min, resulting in two distinct liquid phases. The organic phase was collected to a fresh glass tube with a Pasteur pipette and dried under N₂. Samples were resuspendend in hexane.

Lipids were analyzed by LC-MS/MS using a SCIEX QTRAP 6500⁺ equipped with a Shimadzu LC-30AD (Kyoto, Japan) HPLC system and a 150 \times 2.1 mm, 5 μ m Supelco Ascentis silica column (Bellefonte, PA, USA). Samples were injected at a flow rate of 0.3 ml/min at 2.5% solvent B (methyl tert-butyl ether) and 97.5% Solvent A (hexane). Solvent B is increased to 5% during 3 minutes and then to 60% over 6 minutes. Solvent B is decreased to 0% during 30 seconds while Solvent C (90:10 (v/v) Isopropanol-water) is set at 20% and increased to 40% during the following 11 minutes. Solvent C is increased to 44% during 6 minutes and then to 60% during 50 seconds. The system was held at 60% of solvent C during 1 minutes prior to re-equilibration at 2.5% of solvent B for 5 minutes at a 1.2mL/min flow rate. Solvent D (95:5 (v/v) Acetonitrile-water with 10mM Ammonium acetate) was infused post-column at 0.03ml/min. Column oven temperature was set to 25°C. Data was acquired in positive and negative mode by employing polarity switching during the analysis. Data were acquired using multiple reaction monitoring (MRM) transition for the major, abundant lipid species from all lipid classes. Electrospray ionization source parameters were, GS1 40, Cur 20, source temperature 150 °C, declustering potential 60, and collision energy 25. GS1 and 2 were zero-grade air while Cur and CAD gas was nitrogen. MRM transitions for cholesteryl esters were analyzed using MultiQuant software (SCIEX).

VPA0226 protein purification

One 6mL culture each of CAB2 Δ vpa0226 transformed with pBAD 6His::VPA0226 and CAB2 Δ vpa0226 transformed with pBAD 6His::VPA0226 S153A was grown shaking

overnight at 30°C. Overnight cultures were each used to inoculate 500mL MLB, which was grown shaking at 30°C for three hours to an OD600 = 0.85. Cultures were induced in 0.1% arabinose 8-12 hours shaking at 30°C. Inductions were pelleted by centrifugation at 4°C in a JA10 Beckman & Coulter and supernatant was collected. 6xHis-tagged VPA0226 and VPA0226 S153A were purified from the supernatant using Ni²⁺ affinity purification.

Phospholipase 2 assay

Purified VPA0226 WT and VPA0226 S/A proteins were tested for phospholipase2 (PLA2) activity using EnzCheck phospholipase A2 assay kit according to manufacturer's instructions. Briefly, 0, 0.1, 0.3 and 1 µg of protein was mixed with the proprietary substrate BODIPY PC-A2 in a 100 µl reaction buffer of 50mM Tris-HCl, 100mM NaCl, and 1mM CaCl₂, pH 8.9 in a clear bottom, black 96-well plate and incubated at RT for 30 min, protected from light. Fluorescence was measured using a Clariostar plus plate reader with excitation/emission wavelengths at 460/515. PLA2 from bee venom provided in the kit was used as a positive control.

Liposome assay

Large unilamellar vesicle liposomes containing 50 µMol each of cholesterol:cardiolipin (1',3'-bis[1,2-dioleoyl-sn-glycero-3-phospho]-glycerol) or 50 µMol each of cholesterol:DOPS (1,2-dioleoyl-sn-glycero-3-phospho-L-serine) (Avanti Polar Lipids) were prepared as described previously (43). Briefly, dried lipid films containing lipid mixture were hydrated in 100 µL of 50 mM Tris, pH 7.4, 160 mM KCl by continuous vortexing for 5 min and taken through 5 cycles of freeze- thawing in liquid nitrogen. The resulting liposomes were extruded using an Avanti miniextruder and 100 nm polycarbonate membranes to obtain uniform liposomes. 10 µL of above liposomes were mixed with 5 µg of purified VPA0226 WT or S153A protein in 50 mM Tris, pH 7.4, 160mM KCl plus 1.4% fat free albumin and incubated at 37°C for 1h (16). Reactions were terminated by the addition of chloroform:methanol (2:1 v/v) and the lipids were extracted by Bligh and Dyers method (19) and dissolved in 15 µL of chloroform for TLC analysis. Lipids were separated by TLC using plastic backed silica gel H plates (Sigma)

and a mobile phase system containing petroleum ether: ethyl ether: acetic acid in 90:10:1 ratio. Lipid spots were visualized by exposure to iodine vapor. Cholesterol oleate (Sigma) and above-mentioned lipids were spotted as standards on the TLC plate.

qPCR analysis

Hela cells were transfected with empty vector sf-GFPN1, VPA0226-WT sf-GFPN1 or VPA0226-H/A sf-GFPN1 as described above. 14h post transfection, RNA was isolated from the transfected cells using RNAeasy plus mini kit (Qiagen) according to the manufacturer's instructions. cDNA was generated using the qScript cDNA synthesis kit (Qunatabio). qPCR analysis for gene expression levels was carried out on a CFX384 Touch Real-Time PCR Detection System using PerfeCTa SYBR Green Supermix (Quantabio) and 500nM primers. The primers were designed based on the established database, Primer Bank, PCR primers for Gene Expression Detection and Quantification and were checked for efficiency (44). Relative gene expression level for the target genes was calculated by the ΔC_q method with respect to transcript levels of the housekeeping gene GAPDH.

Propidium Iodide binding assay

Susceptibility of Hela cells to mechanical stress was assessed following the protocol Hela cells transfected with empty vector sf-GFPN1, VPA0226-WT sf-GFPN1 or VPA0226-H/A sf-GFPN1 for 14 h were harvested by scraping the cells into sterile PBS. The cells were washed twice with PBS. 1×10^5 cells were resuspended in water containing 5 μ M propidium iodide (ThermoFisher Scientific) and incubated at room temperature for 10 min. Fluorescence was immediately measured using a Clariostar plus plate reader with excitation/emission wavelengths at 530/620 nm.

Statistical analysis and bioinformatics

All data are given as mean \pm standard deviation from at least 3 independent experiments unless stated otherwise. Each experiment was conducted in triplicate. Statistical analyses were performed by using unpaired, two-tailed Student's t test with

Welch's correction and one-way ANOVA with Turkey's multiple comparison test. A p value of < 0.05 was considered significant.

For sequence similarity-based CLANS clustering, the RP15 representative sequence set of the Lipase_GDSL family (Pfam database ID: PF00657) was used. Sequence redundancy was removed by CD-HIT clustering at 60% sequence identity. Similarities up to BLAST E-value 0.01 were used.

CLANS: <https://www.ncbi.nlm.nih.gov/pubmed/15284097>

CD-HIT: <https://www.ncbi.nlm.nih.gov/pubmed/20053844>

Acknowledgements

We thank members of the Orth lab for their discussions and editing. This work was funded NIH grants R01 GM115188 and RO1 GM113079, Once Upon a Time...Foundation and the Welch Foundation I-1561. Dr. Jeffery G. McDonald is supported by PO1 HL20948. Dr. Jen Liou is a Sowell Family Scholar in Medical Research. Dr. Kim Orth is a Burroughs Welcome Investigator, a Beckman Young Investigator, and a W. W. Caruth, Jr., Biomedical Scholar with an Earl A. Forsythe Chair in Biomedical Science

Competing Interest. None

References

1. Wang, R., Zhong, Y., Gu, X., Yuan, J., Saeed, A. F., and Wang, S. (2015) The pathogenesis, detection, and prevention of *Vibrio parahaemolyticus*. *Front Microbiol* **6**, 144
2. Makino, K., Oshima, K., Kurokawa, K., Yokoyama, K., Uda, T., Tagomori, K., Iijima, Y., Najima, M., Nakano, M., Yamashita, A., Kubota, Y., Kimura, S., Yasunaga, T., Honda, T., Shinagawa, H., Hattori, M., and Iida, T. (2003) Genome sequence of *Vibrio parahaemolyticus*: a pathogenic mechanism distinct from that of *V. cholerae*. *Lancet* **361**, 743-749
3. De Souza Santos, M., and Orth, K. (2019) The Role of the Type III Secretion System in the Intracellular Lifestyle of Enteric Pathogens. *Microbiol Spectr* **7**
4. Zhang, L., Krachler, A. M., Broberg, C. A., Li, Y., Mirzaei, H., Gilpin, C. J., and Orth, K. (2012) Type III effector VopC mediates invasion for *Vibrio* species. *Cell Rep* **1**, 453-460

5. Zhang, L., and Orth, K. (2013) Virulence determinants for *Vibrio parahaemolyticus* infection. *Curr Opin Microbiol* **16**, 70-77
6. de Souza Santos, M., and Orth, K. (2014) Intracellular *Vibrio parahaemolyticus* escapes the vacuole and establishes a replicative niche in the cytosol of epithelial cells. *MBio* **5**, e01506-01514
7. Trosky, J. E., Mukherjee, S., Burdette, D. L., Roberts, M., McCarter, L., Siegel, R. M., and Orth, K. (2004) Inhibition of MAPK signaling pathways by VopA from *Vibrio parahaemolyticus*. *J Biol Chem* **279**, 51953-51957
8. Liverman, A. D., Cheng, H. C., Trosky, J. E., Leung, D. W., Yarbrough, M. L., Burdette, D. L., Rosen, M. K., and Orth, K. (2007) Arp2/3-independent assembly of actin by *Vibrio* type III effector VopL. *Proc Natl Acad Sci U S A* **104**, 17117-17122
9. de Souza Santos, M., Salomon, D., and Orth, K. (2017) T3SS effector VopL inhibits the host ROS response, promoting the intracellular survival of *Vibrio parahaemolyticus*. *PLoS Pathog* **13**, e1006438
10. Trosky, J. E., Li, Y., Mukherjee, S., Keitany, G., Ball, H., and Orth, K. (2007) VopA inhibits ATP binding by acetylating the catalytic loop of MAPK kinases. *J Biol Chem* **282**, 34299-34305
11. Ruiz-Albert, J., Yu, X. J., Beuzon, C. R., Blakey, A. N., Galyov, E. E., and Holden, D. W. (2002) Complementary activities of SseJ and SifA regulate dynamics of the *Salmonella typhimurium* vacuolar membrane. *Mol Microbiol* **44**, 645-661
12. Fredlund, J., and Enninga, J. (2014) Cytoplasmic access by intracellular bacterial pathogens. *Trends Microbiol* **22**, 128-137
13. Wan, Y., Liu, C., and Ma, Q. (2019) Structural analysis of a *Vibrio* phospholipase reveals an unusual Ser-His-chloride catalytic triad. *J Biol Chem*
14. Shinoda, S., Matsuoka, H., Tsuchie, T., Miyoshi, S., Yamamoto, S., Taniguchi, H., and Mizuguchi, Y. (1991) Purification and characterization of a lecithin-dependent haemolysin from *Escherichia coli* transformed by a *Vibrio parahaemolyticus* gene. *J Gen Microbiol* **137**, 2705-2711
15. Banerji, S., Bewersdorff, M., Hermes, B., Cianciotto, N. P., and Flieger, A. (2005) Characterization of the major secreted zinc metalloprotease- dependent glycerophospholipid:cholesterol acyltransferase, PlaC, of *Legionella pneumophila*. *Infect Immun* **73**, 2899-2909
16. Buckley, J. T. (1982) Substrate specificity of bacterial glycerophospholipid:cholesterol acyltransferase. *Biochemistry* **21**, 6699-6703
17. Nawabi, P., Catron, D. M., and Haldar, K. (2008) Esterification of cholesterol by a type III secretion effector during intracellular *Salmonella* infection. *Mol Microbiol* **68**, 173-185
18. Van der Henst, C., Vanhove, A. S., Drebes Dorr, N. C., Stutzmann, S., Stoudmann, C., Clerc, S., Scignari, T., Maclachlan, C., Knott, G., and Blokesch, M. (2018) Molecular insights into *Vibrio cholerae*'s intra-amoebal host-pathogen interactions. *Nat Commun* **9**, 3460
19. Bligh, E. G., and Dyer, W. J. (1959) A rapid method of total lipid extraction and purification. *Can J Biochem Physiol* **37**, 911-917

20. Lambert, D., O'Neill, C. A., and Padfield, P. J. (2005) Depletion of Caco-2 cell cholesterol disrupts barrier function by altering the detergent solubility and distribution of specific tight-junction proteins. *Biochem J* **387**, 553-560
21. Grunze, M., and Deuticke, B. (1974) Changes of membrane permeability due to extensive cholesterol depletion in mammalian erythrocytes. *Biochim Biophys Acta* **356**, 125-130
22. Tallima, H., and El Ridi, R. (2018) Arachidonic acid: Physiological roles and potential health benefits - A review. *J Adv Res* **11**, 33-41
23. Brown, M. S., and Goldstein, J. L. (1997) The SREBP pathway: regulation of cholesterol metabolism by proteolysis of a membrane-bound transcription factor. *Cell* **89**, 331-340
24. Li, P., Rivera-Cancel, G., Kinch, L. N., Salomon, D., Tomchick, D. R., Grishin, N. V., and Orth, K. (2016) Bile salt receptor complex activates a pathogenic type III secretion system. *Elife* **5**
25. Krachler, A. M., Ham, H., and Orth, K. (2011) Outer membrane adhesion factor multivalent adhesion molecule 7 initiates host cell binding during infection by gram-negative pathogens. *Proc Natl Acad Sci U S A* **108**, 11614-11619
26. Falkow, S. (1988) Molecular Koch's postulates applied to microbial pathogenicity. *Rev Infect Dis* **10 Suppl 2**, S274-276
27. Flores-Díaz, M., Monturiol-Gross, L., Naylor, C., Alape-Girón, A., and Flieger, A. (2016) Bacterial Sphingomyelinases and Phospholipases as Virulence Factors. *Microbiol Mol Biol Rev* **80**, 597-628
28. Zhong, Y., Zhang, X.-H., Chen, J., Chi, Z., Sun, B., Li, Y., and Austin, B. (2006) Overexpression, purification, characterization, and pathogenicity of *Vibrio harveyi* hemolysin VHH. *Infect Immun* **74**, 6001-6005
29. Jang, K. K., Lee, Z.-W., Kim, B., Jung, Y. H., Han, H. J., Kim, M. H., Kim, B. S., and Choi, S. H. (2017) Identification and characterization of *Vibrio vulnificus* plpA encoding a phospholipase A(2) essential for pathogenesis. *The Journal of biological chemistry* **292**, 17129-17143
30. Lee, J.-H., Ahn, S.-H., Kim, S.-H., Choi, Y.-H., Park, K.-J., and Kong, I.-S. (2002) Characterization of *Vibrio mimicus* phospholipase A (PhlA) and cytotoxicity on fish cell. *Biochemical and Biophysical Research Communications* **298**, 269-276
31. Lee, S. J., Jung, Y. H., Oh, S. Y., Song, E. J., Choi, S. H., and Han, H. J. (2015) *Vibrio vulnificus* VvhA induces NF- κ B-dependent mitochondrial cell death via lipid raft-mediated ROS production in intestinal epithelial cells. *Cell Death & Disease* **6**, e1655-e1655
32. Pszeny, V., Ehrenman, K., Romano, J. D., Kennard, A., Schultz, A., Roos, D. S., Grigg, M. E., Carruthers, V. B., and Coppens, I. (2016) A Lipolytic Lecithin:Cholesterol Acyltransferase Secreted by *Toxoplasma* Facilitates Parasite Replication and Egress. *J Biol Chem* **291**, 3725-3746
33. Akoh, C. C., Lee, G. C., Liaw, Y. C., Huang, T. H., and Shaw, J. F. (2004) GDSL family of serine esterases/lipases. *Prog Lipid Res* **43**, 534-552
34. Haas, E., and Stanley, D. W. (2007) Phospholipases. in *xPharm: The Comprehensive Pharmacology Reference* (Enna, S. J., and Bylund, D. B. eds.), Elsevier, New York. pp 1-3

35. Aikawa, S., Hashimoto, T., Kano, K., and Aoki, J. (2014) Lysophosphatidic acid as a lipid mediator with multiple biological actions. *The Journal of Biochemistry* **157**, 81-89
36. Nicolaou, A., Mauro, C., Urquhart, P., and Marelli-Berg, F. (2014) Polyunsaturated Fatty Acid-Derived Lipid Mediators and T Cell Function. *Frontiers in Immunology* **5**
37. Park, K. S., Ono, T., Rokuda, M., Jang, M. H., Okada, K., Iida, T., and Honda, T. (2004) Functional characterization of two type III secretion systems of *Vibrio parahaemolyticus*. *Infect Immun* **72**, 6659-6665
38. Zhou, X., Konkel, M. E., and Call, D. R. (2010) Regulation of type III secretion system 1 gene expression in *Vibrio parahaemolyticus* is dependent on interactions between ExsA, ExsC, and ExsD. *Virulence* **1**, 260-272
39. Ritchie, J. M., Rui, H., Zhou, X., Iida, T., Kodama, T., Ito, S., Davis, B. M., Bronson, R. T., and Waldor, M. K. (2012) Inflammation and disintegration of intestinal villi in an experimental model for *Vibrio parahaemolyticus*-induced diarrhea. *PLoS Pathog* **8**, e1002593
40. Gotoh, K., Kodama, T., Hiyoshi, H., Izutsu, K., Park, K. S., Dryselius, R., Akeda, Y., Honda, T., and Iida, T. (2010) Bile acid-induced virulence gene expression of *Vibrio parahaemolyticus* reveals a novel therapeutic potential for bile acid sequestrants. *PLoS One* **5**, e13365
41. Pedelacq, J. D., Cabantous, S., Tran, T., Terwilliger, T. C., and Waldo, G. S. (2006) Engineering and characterization of a superfolder green fluorescent protein. *Nat Biotechnol* **24**, 79-88
42. Blight, E. G., and Dyer, W. J. (1959) A rapid method of total lipid extraction and purification. *Canadian Journal of Biochemistry and Physiology* **37**, 911-917
43. Sreelatha, A., Bennett, T. L., Zheng, H., Jiang, Q. X., Orth, K., and Starai, V. J. (2013) *Vibrio* effector protein, VopQ, forms a lysosomal gated channel that disrupts host ion homeostasis and autophagic flux. *Proc Natl Acad Sci U S A* **110**, 11559-11564
44. Spandidos, A., Wang, X., Wang, H., and Seed, B. (2010) PrimerBank: a resource of human and mouse PCR primer pairs for gene expression detection and quantification. *Nucleic Acids Res* **38**, D792-799

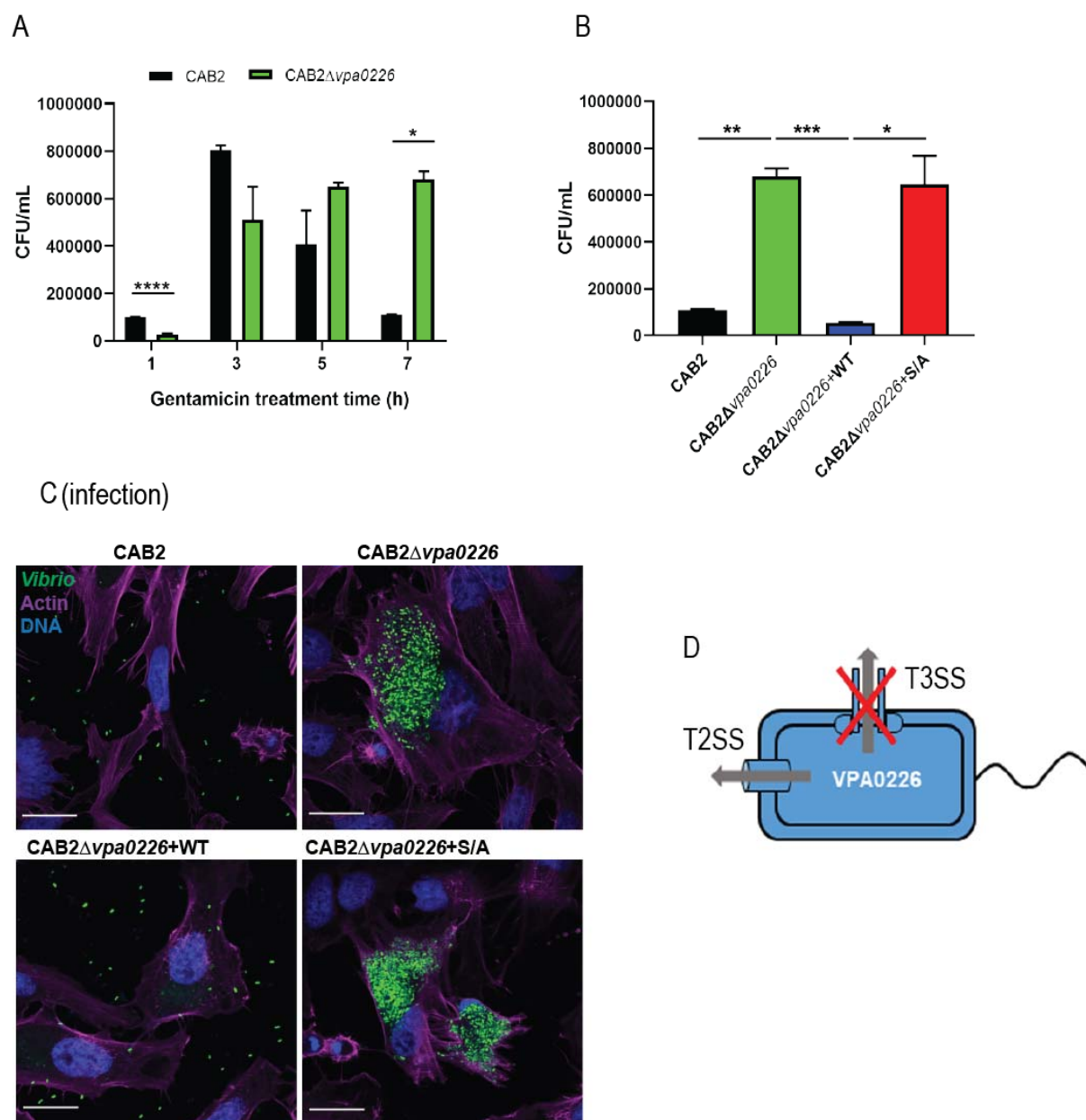


Figure 1. VPA0226 is a type 2 secreted lipase that mediates bacterial egress from the host cell.

(A) HeLa cells were infected with CAB2 or CAB2Δvpa0226 for 1, 3, 5, and 7 hours PGT. Host cell lysates were serially diluted and plated onto MMM agar plates for intracellular bacterial colony counting (CFU/mL). Numbers are expressed as an average of three technical replicates for one of three independent experiments. Error bars represent standard deviation from the mean. Asterisks represent statistical significance

(* = $p < 0.05$, **** = $p < 0.0001$) using Student's t test. **(B)** HeLa cells were infected with CAB2, CAB2 Δ *vpa0226*, CAB2 Δ *vpa0226*+WT, or CAB2 Δ *vpa0226*+S/A for 7 hours PGT. Host cell lysates were serially diluted and plated onto MMM agar plates for intracellular bacterial colony counting (CFU/mL). Numbers are expressed as an average of three technical replicates for one out of three independent experiments. Error bars represent standard deviation from the mean. Asterisks represent statistical significance (* = $p < 0.05$, ** = $p < 0.005$, *** = $p < 0.0005$) using Student's t test. **(C)** Confocal micrographs of HeLa cells infected with GFP-expressing (green) CAB2, CAB2 Δ *vpa0226*, CAB2 Δ *vpa0226*+WT, or CAB2 Δ *vpa0226*+S/A for 7 hours PGT. Host cell actin was stained with Alexa 680-phalloiding (magenta) and DNA was stained with Hoechst (blue). Scale bars = 25 μ m. **(D)** Schematic of VPA0226 secretion through T2SS and not T3SS2.

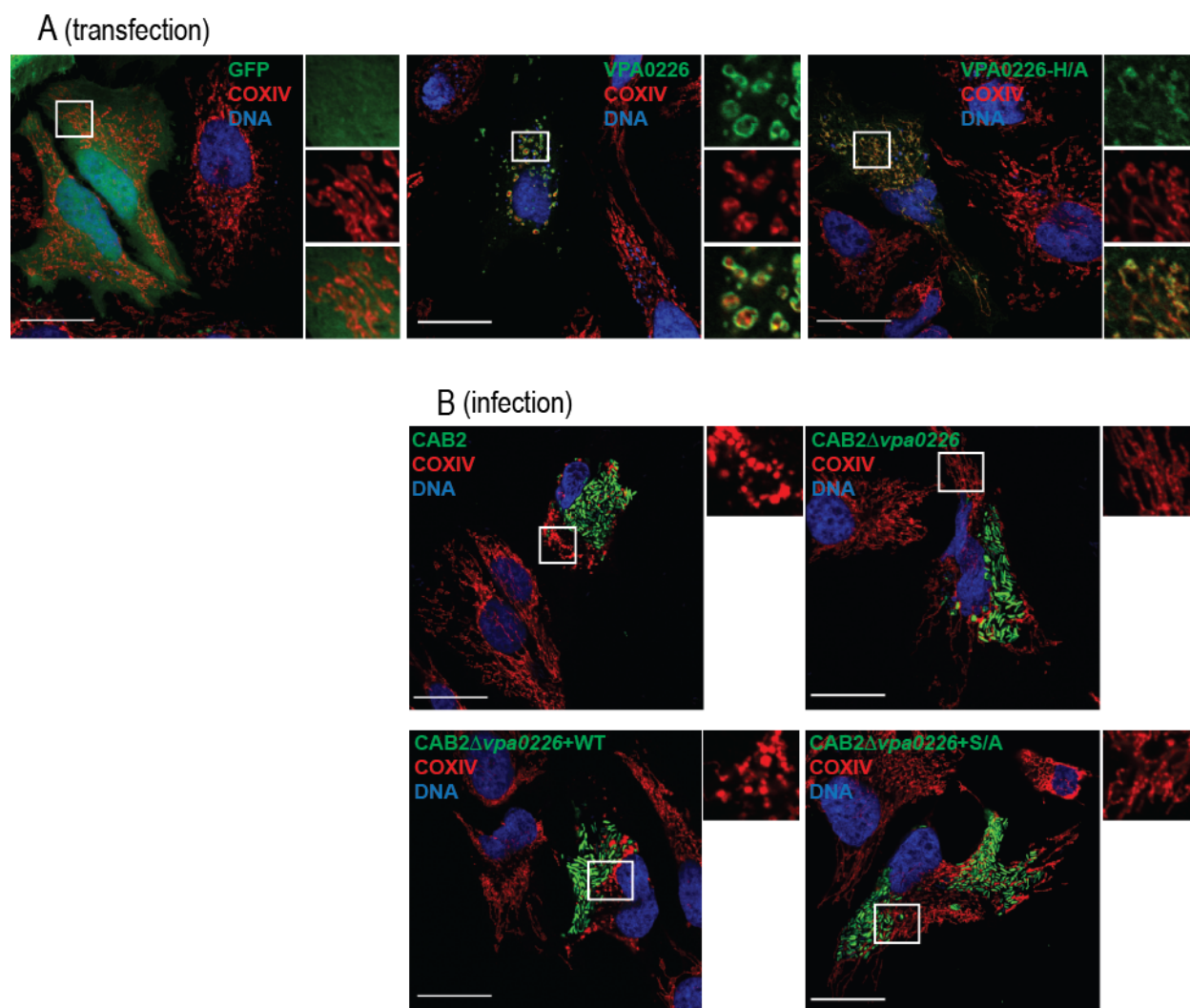


Figure 2. VPA0226 localizes to and fragments mitochondria in the host cell.

(A) Confocal micrographs of HeLa cells transiently transfected with empty vector, VPA0226- or VPA0226-H/A-sfGFPN1 (green) for 14 hours. Mitochondria were stained with anti-COXIV antibody (red) and DNA was stained with Hoechst (blue). Scale bars = 25 μ m. White boxes frame magnified areas. **(B)** Confocal micrographs of HeLa cells infected with GFP-expressing (green) CAB2, CAB2 Δ vpa0226, CAB2 Δ vpa0226+WT, or CAB2 Δ vpa0226+S/A with anti-COXIV antibody (red) and DNA was stained with Hoechst (blue) at 3.5 hours PGT. Scale bars = 25 μ m. White boxes frame magnified areas.

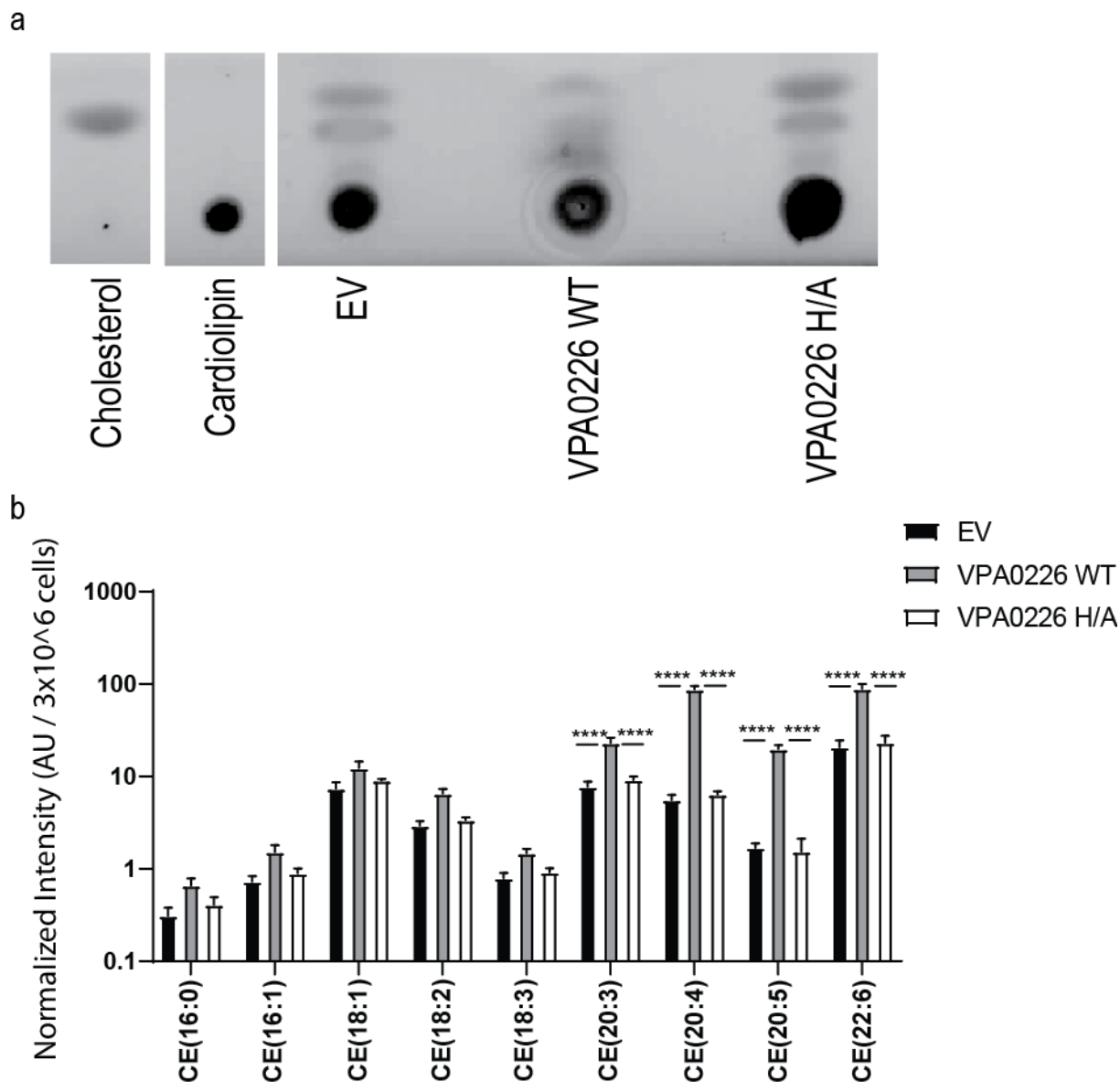


Figure 3. VPA0226 changes lipid profile in cells.

(A) Thin layer chromatography of lipid standards (cardiolipin and cholesterol) and lipids extracted from transfected HeLa cells (empty vector (EV), wildtype VPA0226-sfGFPN1 and VPA0226-H/A-sfGFPN1) **(B)** Analysis of cholesteryl esters extracted from transfected HeLa cells (empty vector (EV), wildtype VPA0226-sfGFPN1 and VPA0226-H/A-sfGFPN1). Numbers are expressed as an average of five technical replicates for one out of three independent experiments. Error bars represent standard deviation from

875 the mean. Asterisks represent statistical significance (**** = $p < 0.0001$) using one-way
876 ANOVA and Turkey's multiple comparison test.

877

878

879

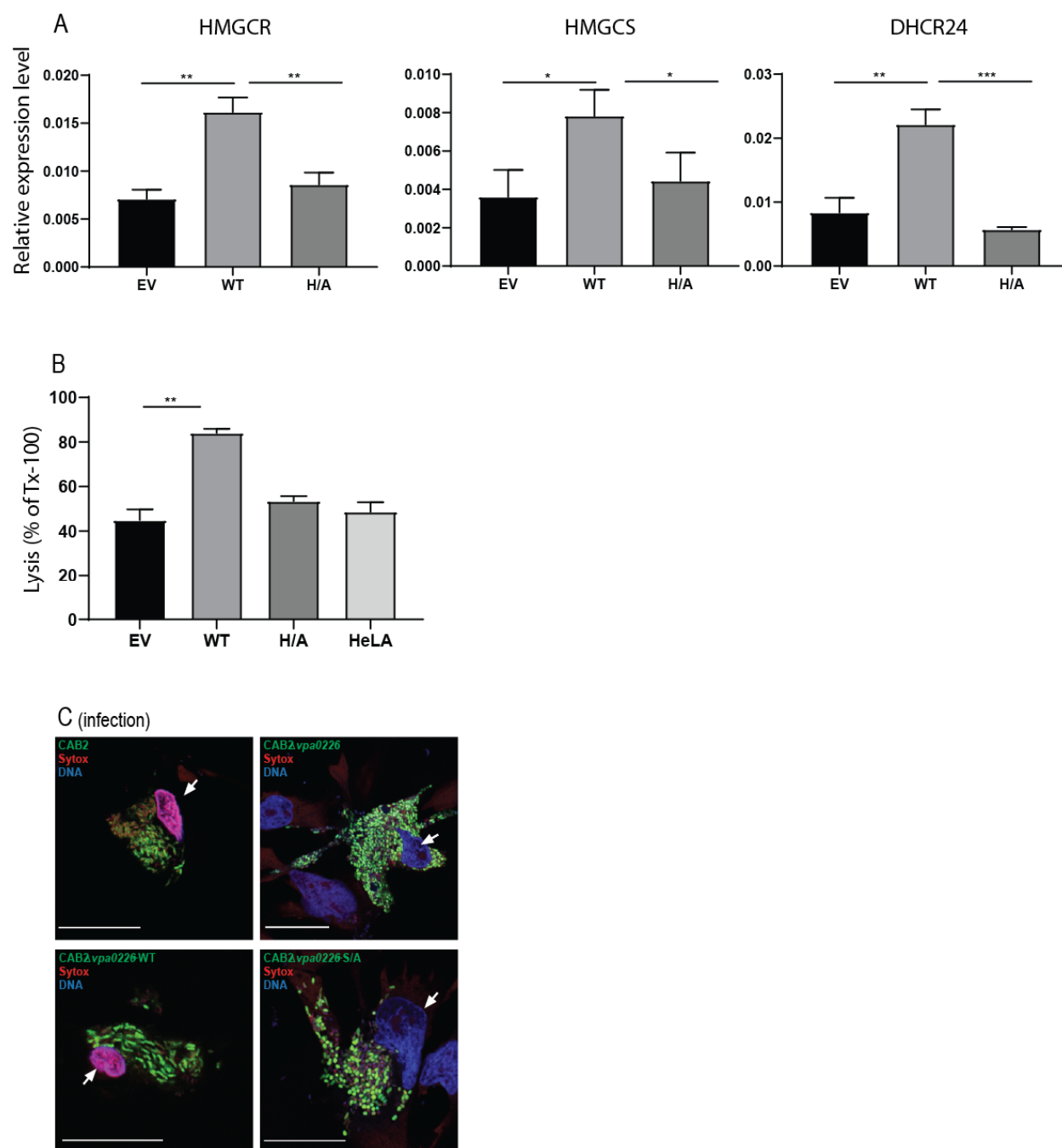


Figure 4. VPA0226 upregulates cholesterol synthesis gene expression in cells and permeabilizes the host cell plasma membrane.

(A) qPCR analysis for relative expression of HMGR, HMGCS and DHCR24, signature genes involved in cholesterol synthesis (SREBP2) pathway in HeLa cells transfected with empty vector (EV), wildtype VPA0226-sfGFPN1 and VPA0226-H/A-sfGFPN1.

Expression was normalized to the house keeping gene GapDH and asterisks represent

statistical significance (* $p < 0.05$, ** $p < 0.005$, *** $p < 0.0005$) using Student's t test. **(B)** Susceptibility to mechanical stress as measured by propidium iodide (PI) binding in transfected HeLa cells (empty vector (EV), wildtype VPA0226-sfGFPN1 and VPA0226-H/A-sfGFPN1), ** $p < 0.005$ using one-way ANOVA and Turkey's multiple comparison test. **(C)** Confocal micrographs of HeLa cells infected with GFP-expressing (green) CAB2, CAB2 $\Delta vpa0226$, CAB2 $\Delta vpa0226$ +WT, or CAB2 $\Delta vpa0226$ +S/A at 5 hours PGT. Cell permeability was assessed by staining with dye Sytox (red), bacteria (green), and DNA (blue, stained with Hoechst). Scale bars = 25 μm . Arrows point to the sytox permeable HeLa cell nuclei in CAB2, and CAB2 $\Delta vpa0226$ +WT, or sytox impermeable nuclei in CAB2 $\Delta vpa0226$, CAB2 $\Delta vpa0226$ +S/A infections.

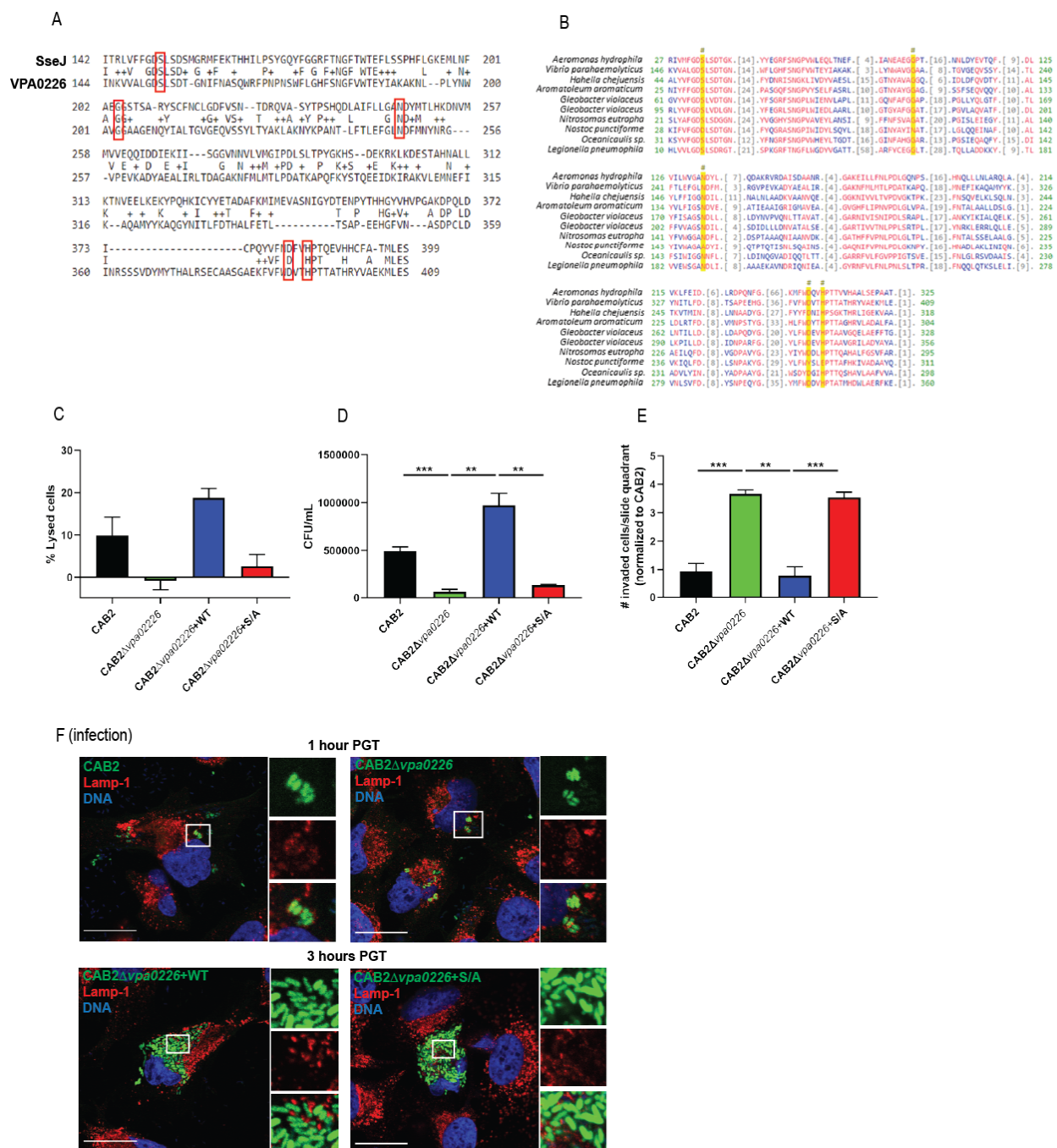


Figure1 - Figure supplement-1. VPA0226 is GCAT lipase that contributes to bacterial cell egress but does not contribute to *V. parahaemolyticus*' escape from its containing vacuole.

(A) Sequence alignment between the *Salmonella* T3SS2 effector SseJ and the *V. parahaemolyticus* lipase VPA0226. Conserved active sites are boxed in red.

(B) Sequence alignment between *V. parahaemolyticus*' VPA0226 and bacterial glycerophospholipid acyltransferases (GCAT). Asterisks and yellow columns indicate conserved active sites. **(C)** HeLa cells were infected with CAB2, CAB2Δ*vpa0226*, CAB2Δ*vpa0226*+WT, or CAB2Δ*vpa0226*+S/A for 7 hours PGT. Cell lysis was assessed by quantification of release of cytosolic lactate dehydrogenase (LDH). Numbers represent the average of nine technical replicates for one out of three independent experiments. Error bars represent standard deviation from the mean. Asterisks represent statistical significance (* = $p < 0.05$, ** = $p < 0.005$, *** = $p < 0.0005$) using Student's t test. **(D)** HeLa cells were infected with CAB2, CAB2Δ*vpa0226*, CAB2Δ*vpa0226*+WT, or CAB2Δ*vpa0226*+S/A for 2 h, after which samples were treated with 100 µg/mL gentamicin for 3 h. Gentamicin was washed away and cells were incubated for additional 3 h. Host cell supernatants were serially diluted and plated onto MMM agar plates for extracellular bacterial colony counting (CFU/mL). Numbers are expressed as an average of three technical replicates for one out of three independent experiments. Error bars represent standard deviation from the mean. Asterisks represent statistical significance (** = $p < 0.005$, *** = $p < 0.0005$) using Student's t test. **(E, relative to Fig. 1c)** Quantification of HeLa cells containing intracellular bacteria per quadrant of slide. Numbers were normalized to CAB2 and are expressed as an average of three independent experiments. Error bars represent standard deviation from the mean. Asterisks represent statistical significance (** = $p < 0.005$, *** = $p < 0.0005$) using Student's t test. **(F)** Confocal micrographs of HeLa cells infected with GFP-expressing (green) CAB2 or CAB2Δ*vpa0226* for 2 h, after which samples were treated with 100 µg/mL gentamicin for 1 or 3 h. Host cell late endosomes were stained with anti-Lamp1 antibody (red) and DNA was stained with Hoechst (blue). Scale bars = 25 µm. White boxes frame magnified areas.

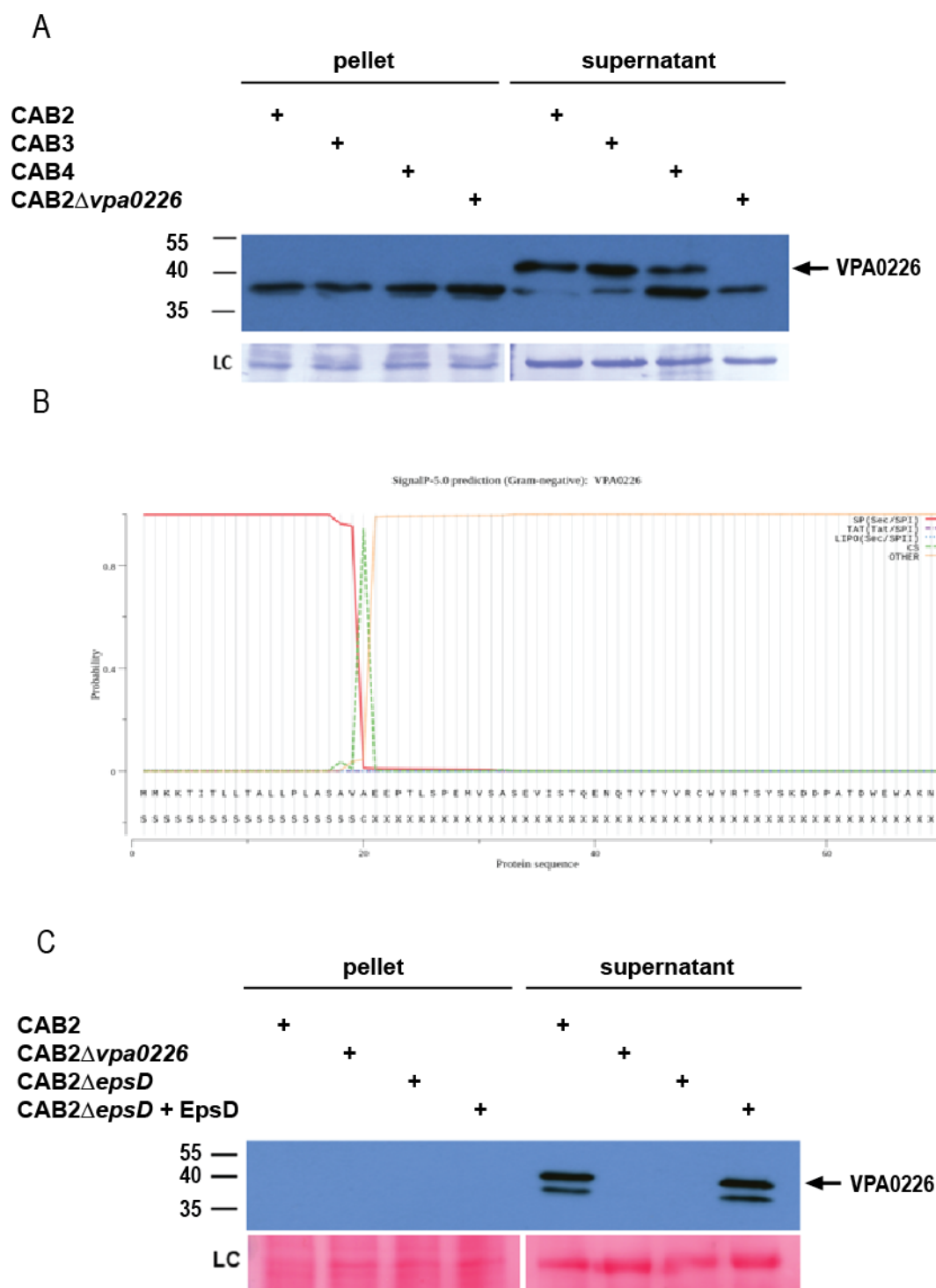


Figure1 - Figure supplement-2. VPA0226 is a T2SS secreted protein.

(A) Expression (pellet) and secretion (supernatant) of VPA0226 from CAB2, CAB3, CAB4 and CAB2Δvpa0226 detected by immunoblotting with anti-VPA0226 antibody.

944 LC: loading control from total bacterial lysate or total secretion media. **(B)** VPA0226
 945 Prediction: Signal peptide (Sec/SPI), (-----) denotes the length of the signal peptide).
 946 Cleavage site between positions 20 and 21 (-----). **(C)** Expression (pellet) and secretion
 947 (supernatant) of VPA0226 from CAB2, CAB2Δvpa0226, CAB2ΔepsD and CAB2ΔepsD
 948 + EpsD detected by immunoblotting with anti-VPA0226 antibody. LC: loading control
 949 from total bacterial lysate or total secretion media.
 950
 951

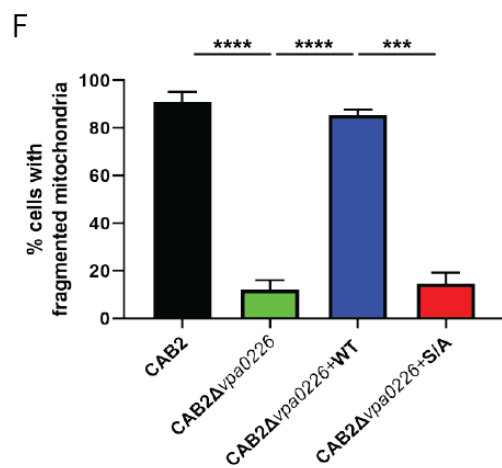
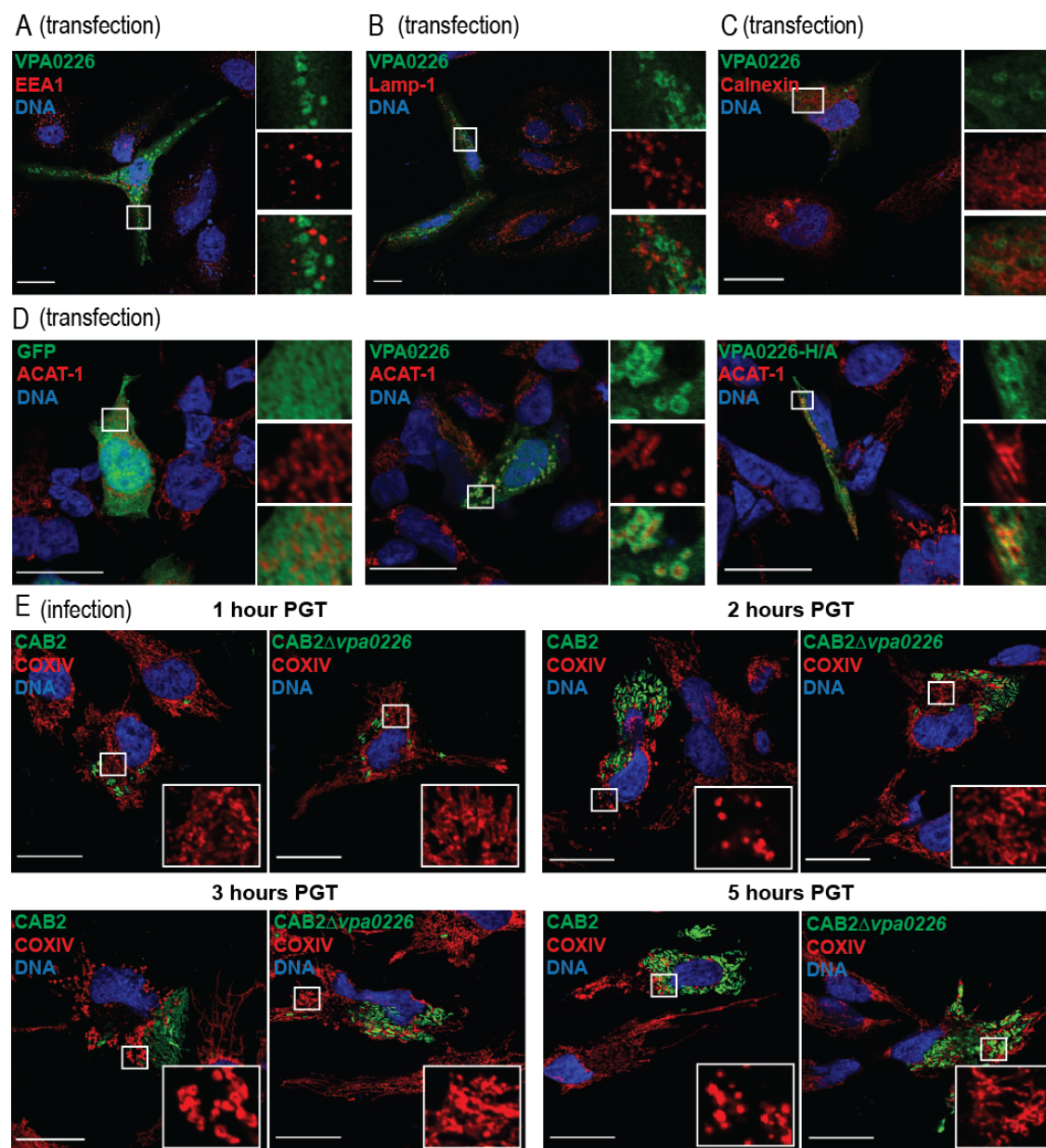


Figure2 - Figure supplement-1. VPA0226 exclusively localizes to the mitochondria.

Confocal micrographs of HeLa cells transiently transfected with VPA0226-sfGFPN1 (green) for 24 h. Early endosomes, late endosomes/lysosomes, and endoplasmic reticulum were stained with **(A)** anti-EEA1, **(B)** anti-lamp1, and **(C)** anti-calnexin antibodies (red), respectively, and DNA was stained with Hoechst (blue). Scale bars = 25 μ m. White boxes frame magnified areas. **(D)** Confocal micrographs of HEK293T cells transiently transfected with empty vector, VPA0226- or VPA0226 H/A-sfGFPN1 (green) for 24 h. Mitochondria were stained with anti-ACAT1 antibody (red) and DNA was stained with Hoechst (blue). Scale bars = 25 μ m. White boxes frame magnified areas. (e) Confocal micrographs of HeLa cells infected with GFP-expressing (green) CAB2, CAB2 Δ *vpa0226*, CAB2 Δ *vpa0226*+WT, or CAB2 Δ *vpa0226*+S/A with anti-COXIV antibody (red) and DNA was stained with Hoechst (blue) at 1, 2, 3 and 5 hours PGT. Scale bars = 25 μ m. White boxes frame magnified areas. (f) Quantification of HeLa cells exhibiting fragmented mitochondria. Numbers are expressed as an average of three independent experiments for 150 cells counted for each sample. Error bars represent standard deviation from the mean. Asterisks represent statistical significance (** = $p < 0.005$).

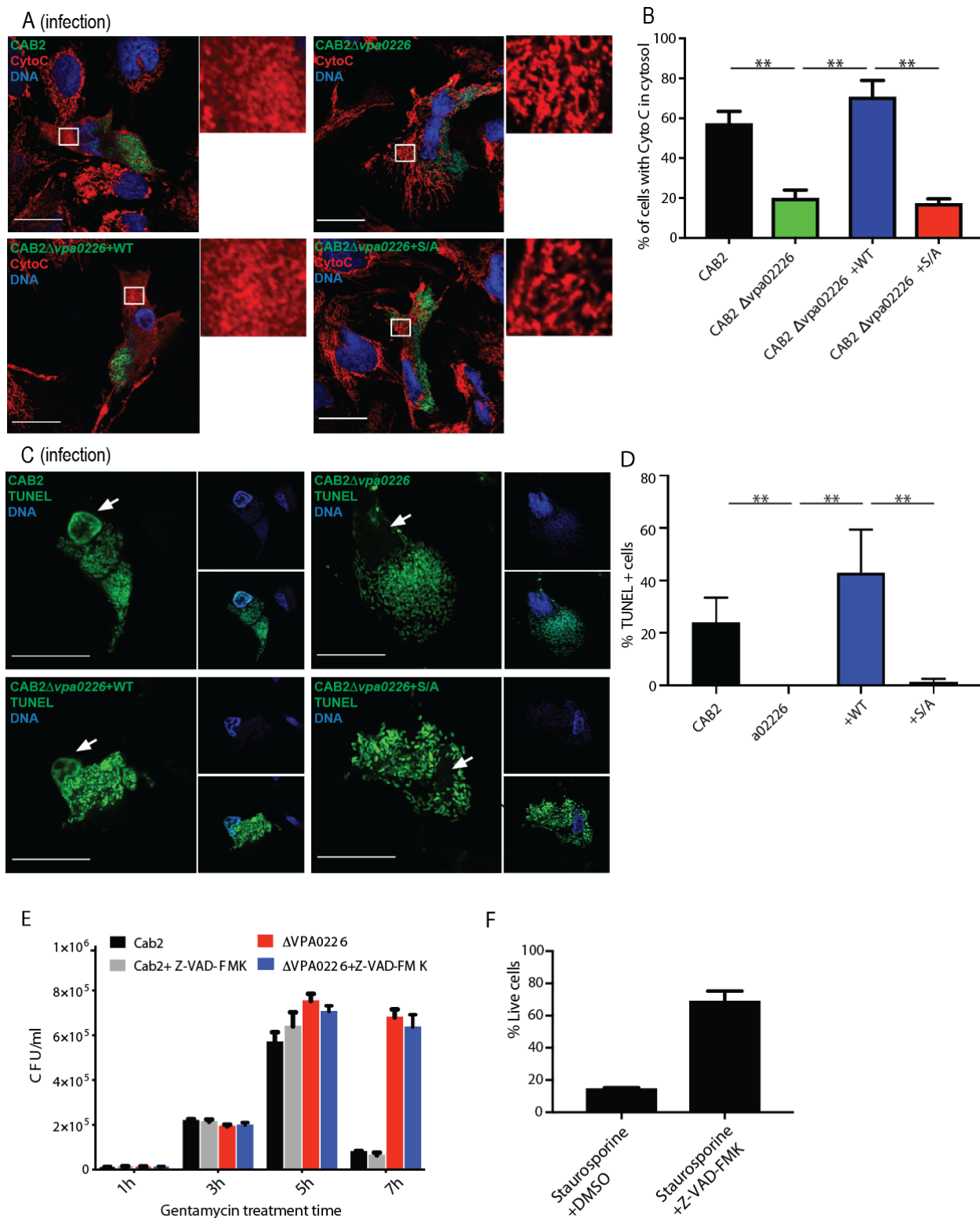


Figure2 - Figure supplement-2. Bacterially invaded cells display apoptotic signatures in a VPA0226-dependent manner.

(A) Confocal micrographs of HeLa cells infected with GFP-expressing (green) CAB2, CAB2Δ*vpa0226*, CAB2Δ*vpa0226*+WT, or CAB2Δ*vpa0226*+S/A tested for release of Cytochrome C (Cyto C) from the mitochondria into the cytosol was assessed by staining of Cyto C with anti-Cytochrome C antibody (red) and DNA was stained with Hoechst (blue) at 5 hours PGT. Scale bars = 25 μm. White boxes frame magnified areas. **(B, relative to A)** Quantification of HeLa cells exhibiting cytosolic CytoC. Numbers are expressed as an average of three independent experiments for 150 cells counted for each sample. Error bars represent standard deviation from the mean. Asterisks represent statistical significance (** = p<0.005). **(C)** Confocal micrographs of HeLa cells infected with GFP-expressing (green) CAB2, CAB2Δ*vpa0226*, CAB2Δ*vpa0226*+WT, or CAB2Δ*vpa0226*+S/A followed by TUNEL staining (green) of host cell nuclei and DNA staining with Hoechst (blue) at 5 hours PGT. Arrows point to TUNEL positive or negative nuclei. Scale bars = 25 μm. **(D, relative to C)** Quantification of HeLa cells positive for TUNEL staining. Numbers are expressed as an average of three independent experiments for 150 cells counted for each sample. Error bars represent standard deviation from the mean. Asterisks represent statistical significance (* = p<0.05). **(E)** HeLa cells were infected with CAB2 or CAB2Δ*vpa0226* for 2 h, in the absence or presence of 50 μM Z-VAD-FMK. Next, samples were treated with 100 μg/mL gentamicin for 1, 3, 5, and 7 h, in the absence or presence of Z-VAD-FMK. Host cell lysates were serially diluted and plated onto MMM agar plates for intracellular bacterial colony counting (CFU/mL). **(F)** HeLa cells were treated with 1.2μM staurosporine for 24 hours in the absence or presence of 50μM Z-VAD-FMK and cell viability was assessed by staining with Trypan Blue.

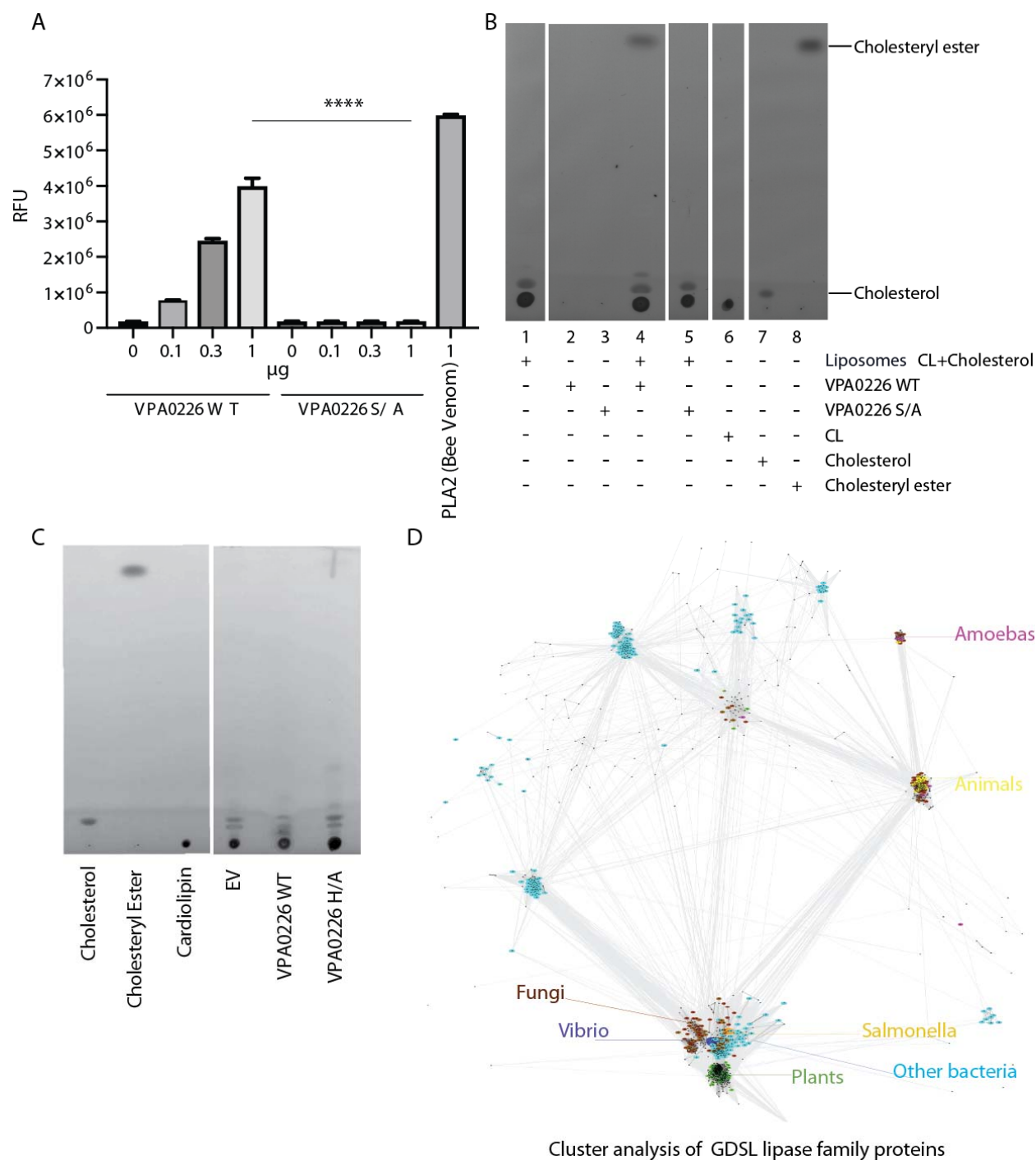


Figure3 - Figure supplement-2.VPA0226 displays phospholipase 2 (PLA 2) activity.

(A) Increasing amounts of purified VPA0226WT or catalytically inactive S/A version were incubated with the fluorogenic PLA2 specific substrate BODIPY PC-A2 (EnzCheck

Phospholipase A2 Assay kit, Invitrogen) for 30 min at RT and fluorescence was measured at Ex/Em 460/515 nm. Error bars represent standard deviation from the mean. Asterisks represent statistical significance (* = $p < 0.05$, *** = $p < 0.0005$) using one-way ANOVA and Turkey's multiple comparison test. **(B)** Thin layer chromatography of lipids extracted from the liposome assay demonstrating the formation of esterified cholesterol in reactions containing cardiolipin (CL) and cholesterol liposomes incubated with wildtype VPA0226 (lane 4). For standards, 10 μ g each of CL, cholesterol and cholesteryl ester were loaded on TLC plate (lanes 6, 7 and 8 respectively). **(C)** Thin layer chromatography of lipid standards (cardiolipin, cholesteryl ester and cholesterol) and lipids extracted from transfected HeLa cells (empty vector (EV), wildtype VPA0226-sfGFPN1 and VPA0226-H/A-sfGFPN1). **(D)** CLANS graph depicts sequence similarity relationships between GDSL lipases, by clustering protein sequences according to pairwise BLAST-derived scores. 1500 representative sequences of representatives of the Lipase_GDSL family shown. Coloring by taxonomy: *Vibrio* – dark blue, *Salmonella* – orange, other bacteria – cyan, fungi – brown, plants – green, animals – yellow, amoebas – magenta.